Research Square

Preprints are preliminary reports that have not undergone peer review.
They should not be considered conclusive, used to inform clinical practice,
or referenced by the media as validated information.

Hydrogen Isotope Effect on Self-Organized Radial Electric Field Criticality During Electron Internal Transport Barrier Formation in Toroidal Plasmas

Tatsuya Kobayashi (kobayashi.tatsuya@nifs.ac.jp)
National Institute for Fusion Science
Akihiro Shimizu
National Institute for Fusion Science
Masaki Nishiura
National Institute for Fusion Science
Takeshi Ido
Kyushu University
Shinsuke Satake
National Institute for Fusion Science
Tokihiko Tokuzawa
National Institute for Fusion Science
Toru Tsujimura
National Institute for Fusion Science
Kenichi Nagaoka
National Institute for Fusion Science
Katsumi Ida
National Institute for Fusion Science

Research Article

Keywords: Hydrogen, isotope effect, electric field, plasmas

Posted Date: December 10th, 2021

DOI: https://doi.org/10.21203/rs.3.rs-1143949/v1

License: This work is licensed under a Creative Commons Attribution 4.0 International License.
Read Full License

Hydrogen isotope effect on self-organized radial electric field criticality during electron internal transport barrier formation in toroidal plasmas

T. Kobayashi[1,2,*], A. Shimizu[1,2], M. Nishiura[1], T. Ido[3], S. Satake[1,2], T. Tokuzawa[1,2], T. Ii Tsujimura[1], K. Nagaoka[1], and K. Ida[1,2]

[1]National Institute for Fusion Science, National Institutes of Natural Sciences, Toki 509-5292, Japan
[2]The Graduate University for Advanced Studies, SOKENDAI, Toki 509-5292, Japan
[3]Research Institute for Applied Mechanics, Kyushu University, Kasuga 816-8580, Japan
[*]kobayashi.tatsuya@nifs.ac.jp

ABSTRACT

Self-organized structure formation in magnetically confined plasmas is one of the most attractive subjects in modern experimental physics. Nonequilibrium media are known to often exhibit phenomena that cannot be predicted by superposition of linear theories. One representative example of such phenomena is the hydrogen isotope effect in fusion plasmas, where the larger the mass of the hydrogen isotope fuel is the better the plasma confinement becomes, contrary to what simple scaling models anticipate. In this article, threshold condition of a plasma structure formation is shown to have a strong hydrogen isotope effect. To investigate the underlying mechanism of this isotope effect, the electrostatic potential is directly measured by a heavy ion beam probe. It is elucidated that the positive radial electric field structure can be driven by less input power normalized by plasma density in plasmas with larger isotope mass across the structure formation.

Introduction

A long-standing open question in the magnetically confined plasma study is the hydrogen isotope effect:[1–5] the heavier the fuel particles are the better the confinement becomes, contrary to what simple scaling models anticipate. The hydrogen isotope effect has been classically assessed by means of the global confinement time scaling or the local diffusivity. When evaluating such parameters, it is usually inevitable to rely on specific assumptions in heating profile calculation or transport models, which can be sources of uncertainty. Moreover, the hydrogen isotope effect in global or local transport coefficients is not always distinct but can be marginal particularly in stellarators.[5] Therefore, a large scale statistics is necessary for drawing a conclusive trend, which can hamper interpretation on detailed underlying process.

The hydrogen isotope effect is also known to be evident in the edge transport barriers (ETBs)[4,6–8] or the internal transport barriers (ITBs),[9] where the threshold condition for the transition is eased in plasmas with larger ion mass. The transport barrier criticality can be qualitatively defined without any model assumption, therefore an experiment-driven discussion for unveiling the underlying physics of the hydrogen isotope effect is possible. Furthermore, as the future thermonuclear fusion plant is currently planned to be operated with the tritium-deuterium mixture fuel and with transport barriers, understanding of the background mechanism of the hydrogen isotope effect is important for projecting the reactor plasma performance. When the transport barriers emerge, a localized radial electric field structure is spontaneously formed by the quasi-neutral plasma,[10] which is believed to suppress the anomalous turbulent transport. Direct measurement of the radial electric field in systematic isotope experiments is therefore a key factor for resolving this issue, but has been challenging for a long time.

In this article, the hydrogen isotope effect on the ITB criticality in the Large Helical Device (LHD) stellarator is elaborated, focusing upon the ITB in the electron temperature profile, the so-called electron ITB. The threshold value in the input power normalized by plasma density for triggering the electron ITB is found to be lowered in plasmas with larger isotope mass. Heavy ion beam probe (HIBP) reveals that the radial electric field transition at the ITB formation is induced by a lower input power normalized by density in plasmas with heavier ions. The fact that the self-organized radial electric field criticality has a susceptibility to plasma ion mass can be a missing piece in resolving the hydrogen isotope effect.

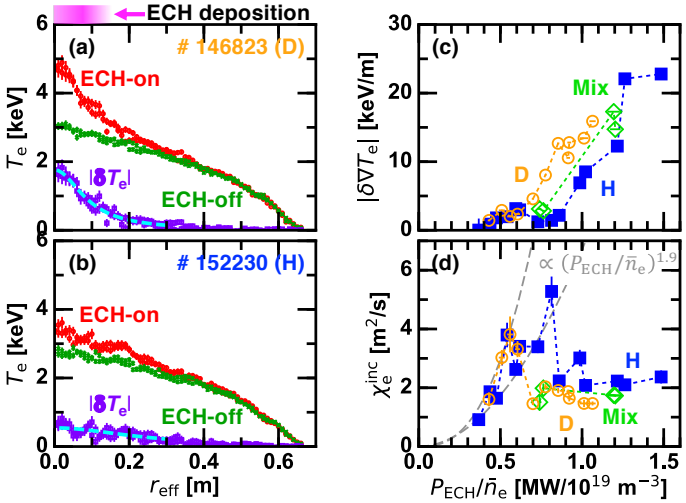

Figure 1. Radial profiles of the electron temperature when the ECH is applied and not applied for (a) deuterium plasmas and (b) hydrogen plasmas; (c) the peak-to-peak modulation amplitude of the electron temperature gradient and (d) the incremental heat diffusivity as a function of the applied ECH power normalized by the line averaged density. Magnitude of the profile variation $|\delta T_e|$ is plotted by purple symbols with the Lorentzian fit in (a) and (b).

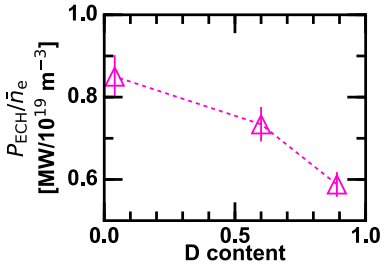

Figure 2. Deuterium content dependence of the threshold value of ECH power normalized by the line averaged density for the ITB transition.

Results

Experimental set-up

Hydrogen isotope effect in the electron ITB is dynamically investigated by means of an input power modulation experiment in LHD (see Methods for details). Electron cyclotron resonance heating (ECH) focused at the torus core is modulated with the peak-to-peak amplitude of $P_{ECH} = 1$ MW and the frequency of $f_{mod} = 23$ Hz. In order to assess the threshold input power normalized by plasma density for the ITB formation, a shot-to-shot basis density scan is performed in deuterium (D) dominant plasmas, hydrogen (H) dominant plasmas, and D-H mixed plasmas. Here, the D content determined by a passive spectroscopy is maintained approximately constant at 89 %, 4 %, and 60 %, respectively, during the density scan.

Hydrogen isotope effect in ITB threshold

Evolution of the electron temperature (T_e) profile is measured by the Thomson scattering system.[11] Figures 1 (a) and (b) compare T_e profiles in the ECH-on and -off phases in D and H discharges at the line averaged density of $\bar{n}_e \sim 1.2 \times 10^{19}$ m^{-3}. Here, r_{eff} is the effective minor radius of the torus. In the D plasma [Fig. 1 (a)], central T_e drastically increases when the ECH is applied while the H plasma shows a marginal increment [Fig. 1 (b)]. The profile variation is fitted by the Lorentzian function $A\Delta r_{eff}\left[r_{eff}^2 + \Delta r_{eff}^2\right]^{-1}$ as shown by dashed curves in Figs. 1 (a) and (b). The peak-to-peak modulation amplitude in T_e gradient, $|\delta \nabla T_e| \sim -0.65 \times A\Delta r_{eff}^{-2}$, is plotted as a function of the applied ECH power normalized by the line averaged density $P_{ECH}/\bar{n}_e$ in Fig. 1 (c). When $P_{ECH}/\bar{n}_e$ is low, $|\delta \nabla T_e|$ remains low as well. As $P_{ECH}/\bar{n}_e$ is increased, $|\delta \nabla T_e|$ begins to monotonically increase once $P_{ECH}/\bar{n}_e$ exceeds threshold values that depend on the D content.

In Fig. 2, the threshold values are plotted as a function of the D content by taking the value of $P_{ECH}/\bar{n}_e$ at which $|\delta \nabla T_e|$ surpasses 2.5 keV/m. Error bars in the threshold diagram is mainly consequent upon an imperfect reproducibility among

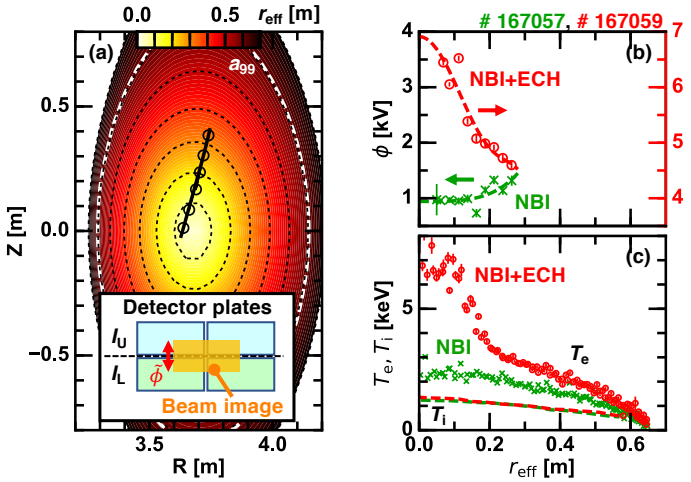

Figure 3. (a) Configuration of HIBP projected on the vertically-elongated poloidal cross-section; radial profiles of (b) the electrostatic potential and (c) the electron and ion temperatures; and (insert) schematic of the HIBP detector plates.

discharges, i.e., vertical scatters of points in Fig. 1 (c). The threshold value in $P_{ECH}/\bar{n}_e$ is found to monotonically decay as the D content is increased. Eased threshold condition for the different types of transport barriers with larger ion mass is ubiquitously observed in various torus plasmas including tokamaks and stellarators,[4,6–9] implying existence of an analogous underlying physics possibly related to the radial electric field drive. Note that the energy flow from electrons to ions is less than 40 kW, which is negligibly small and plays a minor role for the threshold condition.

Local transport property is examined through the electron thermal diffusivity obtained in a perturbative manner, the so-called incremental diffusivity $\chi_e^{inc} \equiv |\delta q_e|/n_e|\delta\nabla T_e|$, where $|\delta q_e|$ is the heat flux variation having the transport time scale and n_e is the electron density. The nonlocal part of the electron heat flux was almost insensitive to the D content.[12] Figure 1 (d) displays $P_{ECH}/\bar{n}_e$ dependence of χ_e^{inc} at $r_{eff} = 0.15$ m. In the lower $P_{ECH}/\bar{n}_e$ regime, χ_e^{inc} increases with $P_{ECH}/\bar{n}_e$. The upper and lower envelopes of the data points are found to be proportional to $(P_{ECH}/\bar{n}_e)^{1.9}$, as shown by grey dashed curves. Gradual confinement degradation as the density is lowered is a common feature of stellarators, and, for instance, is seen in the energy confinement time scaling.[13] In the larger $P_{ECH}/\bar{n}_e$ regime, χ_e^{inc} stays off from the $(P_{ECH}/\bar{n}_e)^{1.9}$ trend, and is maintained low. Those two regimes correspond to non-ITB and ITB regimes, respectively, and the transition threshold value of $P_{ECH}/\bar{n}_e$ clearly depends on the D content, as discussed above.

Electrostatic potential measurement by HIBP

The electron ITB in stellarators is frequently accompanied by a localized positive radial electric field (E_r) structure at the core,[14–17] which is primarily induced through the neoclassical process. Therefore, the electron ITB in stellarators is sometimes referred to as the core electron root confinement (CERC). In order to investigate the role of E_r on the isotope effect in the electron ITB threshold, direct measurement of the electrostatic potential (ϕ) at the plasma core is performed by means of HIBP.[18] HIBP in LHD provides a single point measurement. To obtain the radial profile, the measurement position is scanned either in the 10 Hz reciprocation manner or in a shot-to-shot manner, as shown by the thick curve or the open circles in Fig. 3 (a), respectively. Here, $a_{99} \sim 0.6$ m is the plasma edge in which 99 % of the electron kinetic energy is confined. The local electrostatic potential is translated into the probe beam image position on detector plates [Fig. 3 (a) insert], which are located in the energy analyzer. Current flowing through the lower and upper detector plates, I_L and I_U, respectively, are recorded as the raw HIBP data. The electrostatic potential is given as $\phi = CI_{diff}I_{HIBP}^{-1}$, where $I_{diff} = I_L - I_U$ and $I_{HIBP} = I_L + I_U$ are the HIBP difference current and the HIBP total current, respectively, and C is the proportionality factor.

As an example, radial profile of ϕ measured by HIBP in low density ($\bar{n}_e \sim 0.8 \times 10^{19}$ m^{-3}) stationary hydrogen discharges is shown. Figure 3 (b) shows ϕ profiles in a balanced NB discharge and a stationary ECH superposed discharge measured by a reciprocation position scan. Figure 3 (c) exhibits the electron and ion temperature profiles, where the electron ITB is formed in the ECH superposed discharge. It is evident that ϕ profile with a strong negative gradient, i.e., positive E_r, emerges in the core when the ITB is formed. This positive E_r is likely ascribed to the electron root solution in the neoclassical transport balance as described in.[14–17] Meanwhile, the non-ITB plasma has an almost flat ϕ profile in the core, which corresponds to the ion root solution.

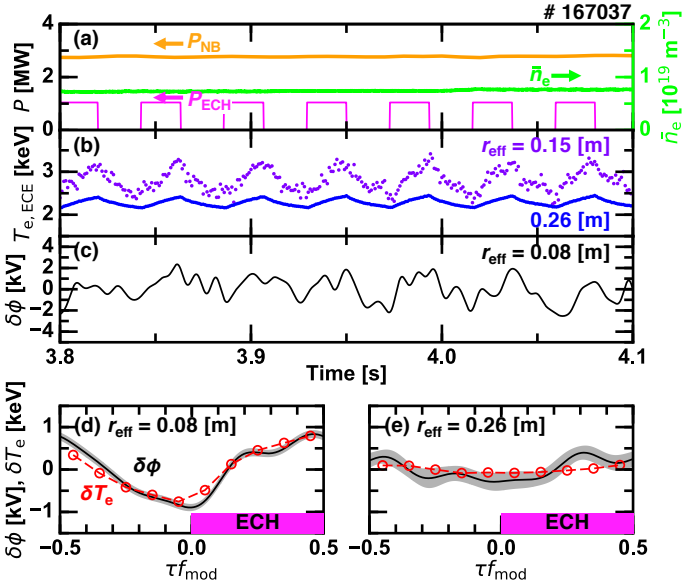

Figure 4. Time evolutions of (a) the heating powers and the line averaged electron density, (b) the electron temperature, and (c) the core electrostatic potential with a 100 Hz low-pass filter; and conditionally averaged electrostatic potential and electron temperature (d) inside and (e) outside the ITB.

Hydrogen isotope effect in radial electric field criticality

HIBP measurement is applied to the ECH modulation discharge to study the critical behavior in E_r across the ITB formation. Aiming at capturing a marginal response in ϕ particularly in higher density discharges discussed below, the measurement position is fixed during the discharge. The radial profile of the ϕ modulation amplitude is obtained in a shot-to-shot HIBP position scan. Figure 4 (a) illustrates the time evolution of a low density hydrogen target discharge. The ECH modulation is applied on the nearly stationary plasma. Figure 4 (b) shows the time evolutions of T_e inside ($r_{eff} = 0.15$ m) and outside ($r_{eff} = 0.26$ m) the ITB measured by ECE radiometers. Modulation amplitude drastically varies across the ITB, corresponding to the localized confinement improvement. Oscillations synchronizing with the 23 Hz ECH modulation are also observed in ϕ variation in the core region [Fig. 4 (c)].

In order to extract the repetitive nature of ϕ variation, the conditional averaging is performed as $\hat{\phi}(\tau) = N^{-1}\sum_{i=1}^{N}\phi(t_i+\tau)$, where $|\tau| < T/2$ and $T = f_{mod}^{-1}$ is the period of the ECH modulation. The value t_i indicates the i-th turn-on time of ECH and N is the total number of the modulation. Figures 4 (d) and (e) show the conditionally averaged ϕ signals at $r_{eff} = 0.08$ m and 0.26 m, i.e., inside and outside the ITB, respectively. In addition, reconstructed T_e variation measured by the Thomson scattering system[19] are overlaid. Inside the ITB, ϕ and T_e simultaneously increase when the ECH is applied, while outside their modulation amplitudes are much smaller. This oscillation amplitude difference in ϕ is indicative of the existence of E_r oscillation that plays a role for the electron ITB formation. It is worthwhile to note that there is an asymmetry in time evolutions of ϕ and T_e, i.e., a stepwise increase and a nearly linear decay. The ITB begins to form at the moment of the ECH application, and quickly saturates making the step-like waveform. When the ECH is terminated, the ITB slowly weakens and eventually returns to the non-ITB plasma.

Figures 5 (a) and (b) compare the conditionally averaged ϕ at different radial positions in D and H low density plasmas of $\bar{n}_e \sim 0.8\times10^{19}$ m^{-3}. The oscillation amplitude gradually decays in the radially outward direction in H plasmas, while it stays nearly unchanged in D plasmas. In order to more distinctly quantify this difference in D and H plasmas, the radial profile of the peak-to-peak ϕ oscillation amplitude for the fundamental modulation frequency component (23 Hz) is shown in Fig. 5 (c). Although the oscillation amplitude is approximately equivalent at the core, its radial extent in D plasmas is wider than that in H plasmas. The E_r peak locations in H and D plasmas are approximately at $r_{eff} \sim 0.2$ m and $r_{eff} \sim 0.3$ m, respectively. A stronger but more localized E_r structure at the ITB region is seemingly excited in H plasmas in contrast to a moderate and wider structure peaked at slightly outer radius in D plasmas. Figure 5 (d) shows T_e variation by the ITB formation. The location where the electron temperature gradient modulation is largest is $r_{eff} \sim 0.1$ m, which is clearly inner than the E_r peak location. D plasmas have a stronger ITB with a slightly wider radial extent. Since E_r is zero in the core by definition, the $E\times B$ flow shear at the ITB location is estimated as $E_r^{peak}/r_{eff}^{peak}$ in the lowest order approximation, where E_r^{peak} and r_{eff}^{peak} are the peak value of E_r and the peak radius, respectively. Therefore, the $E\times B$ flow shear might be stronger in H plasmas due to

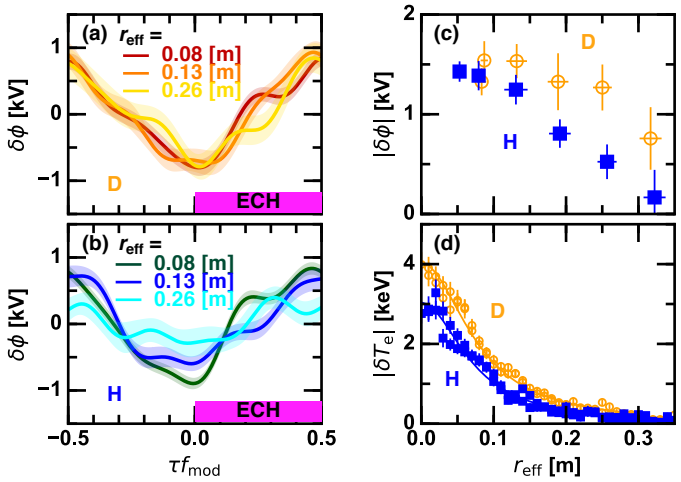

Figure 5. Conditionally averaged electrostatic potentials at various radii for (a) deuterium plasmas and (b) hydrogen plasmas; and radial profiles of the peak-to-peak modulation amplitude in (c) the electrostatic potential and (d) the electron temperature.

larger $E_r^{\rm peak}$ and smaller $r_{\rm eff}^{\rm peak}$. Nevertheless, the resultant ITB is stronger in D plasmas, indicating that the $E \times B$ flow shear paradigm is insufficient for describing the observation. Phenomenologically, a wide radial extent of the positive E_r structure and its shear in D plasmas seem to be more effective for transport suppression and significant ITB formation, rather than the large but localized structure in H plasmas. Importance of positive E_r in diminishing the zonal flow damping is argued in,[20] which can be an interpretation of this observation. According to this model, the zonal flow is a hidden key factor, although its detection in the core is still challenging. Enhancement of the zonal flow activity in D plasmas was experimentally addressed in.[21]

Regardless of the radial gradient scale, the ϕ modulation amplitude at the plasma core is a good proxy for the integrated magnitude of the positive radial electric field modulation. Therefore, response in ϕ to the ECH modulation at the plasma core is explored in the density scan experiment to discuss the underlying mechanism of the isotope effect in the ITB threshold. A diagnostic difficulty for this experiment is that the HIBP signal intensity (total current $I_{\rm HIBP}$) exponentially decays as the density is increased. In such a low signal intensity case, the value of $\phi \propto I_{\rm diff} I_{\rm HIBP}^{-1}$ can be uncertain because of small value in the denominator. In order to settle this problem, the HIBP difference current $I_{\rm diff}$ is used as a proxy of local ϕ. Moreover, level of ϕ response to the ECH modulation pulse is statistically characterized as $\gamma^2 \sin\alpha$, where γ^2 and α are the squared cross coherence and the cross phase between $I_{\rm diff}$ and $P_{\rm ECH}$, respectively. If ϕ modulation is induced by the ECH modulation, α must be $\pi/2$ as shown in Fig. 4 and Fig. 5. Figures 6 (a) and (d) show $\gamma^2 \sin\alpha$ at the modulation ECH frequency of 23 Hz plotted against $P_{\rm ECH}/\bar{n}_{\rm e}$ for D and H plasmas. An example of the frequency spectrum is given in the insert in Fig. 6 (d). In both cases $\gamma^2 \sin\alpha$ decays as $P_{\rm ECH}/\bar{n}_{\rm e}$ is decreased ($\bar{n}_{\rm e}$ is increased).

The decay in γ^2 can be caused either due to disappearance of ϕ modulation in the core or due to deteriorated signal-to-noise ratio. The latter possibility is examined through a synthetic data approach. Decay characteristic of γ^2 is estimated using a mimic HIBP difference current $I_{\rm HIBP} \equiv \hat{I}_{\rm HIBP} \sin 2\pi f_{\rm mod} t + {\rm WGN}(\sigma_0)$, where ${\rm WGN}(\sigma_0)$ is the white Gaussian noise with a standard deviation of σ_0. The modulation amplitude $\hat{I}_{\rm HIBP}$ is decayed following the known density dependence, $\hat{I}_{\rm HIBP} = I_0 \exp[-n_{\rm e}/0.55 \times 10^{19}]$, obtained by a dedicated test. The ratio between I_0 and σ_0 is determined in such a way that the γ^2 curve passes through the experimental data points in the low density domain, where ϕ oscillation is unambiguously observed. The synthetically derived squared cross coherence, referred to as $\gamma^2_{\rm max}$, represents the case where the coherence decays only due to the descent in the HIBP signal intensity.

As shown in Fig. 6 (a), the measured value follows $\gamma^2_{\rm max}$ in the entire $P_{\rm ECH}/\bar{n}_{\rm e}$ range in D plasmas. This indicates that ϕ modulation occurs in all the cases in D plasmas and the variation in the coherence is solely due to the declined HIBP signal intensity in higher density range. In contrast, the measured value stays off from the $\gamma^2_{\rm max}$ curve at $P_{\rm ECH}/\bar{n}_{\rm e} \sim 0.8$ MW/10^{19} m^{-3} in H plasmas as displayed in Fig. 6 (d). It turns out that ϕ at the core scarcely responds to the ECH pulse in $P_{\rm ECH}/\bar{n}_{\rm e} < 0.7$ MW/10^{19} m^{-3}. This difference in D and H plasmas is more evident in the relative plot to the synthetic data, $\gamma^2 \sin\alpha/\gamma^2_{\rm max}$, as shown in Figs. 6 (b) and (e). Figures 6 (c) and (f) indicate the peak-to-peak modulation amplitude in $T_{\rm e}$ gradient. H plasmas begin to form the ITB structure at $P_{\rm ECH}/\bar{n}_{\rm e} \sim 0.8$ MW/10^{19} m^{-3}, where ϕ oscillation becomes substantial. In contrast, the ITB in D plasmas is maintained in the entire range of $P_{\rm ECH}/\bar{n}_{\rm e}$ with the meaningful ϕ oscillation. This observation indicates that the critical behavior in the E_r structure formation that depends on the isotope mass plays a dominant role for the isotope

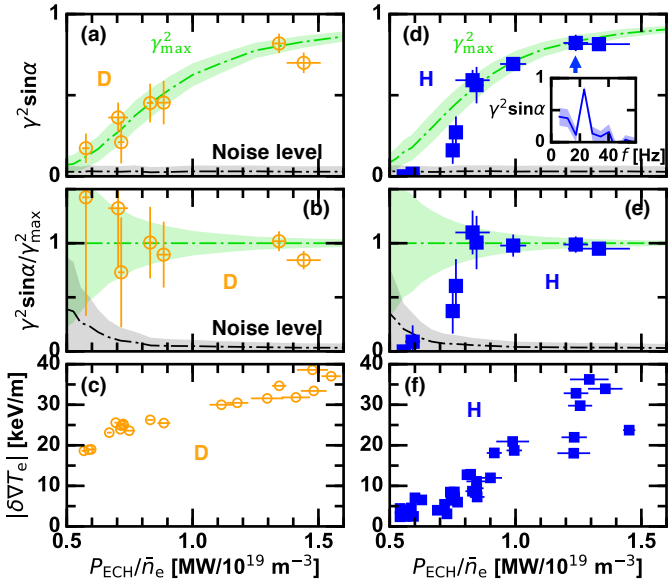

Figure 6. (a,d) Squared coherence of the HIBP difference current with respect to the ECH modulation pulse, (b,e) that normalized by its maximum possible value, and (c,f) the peak-to-peak modulation amplitude of the electron temperature gradient as a function of the applied ECH power normalized by the line averaged density for deuterium plasmas and hydrogen plasmas, respectively; and (insert) squared coherence spectrum for a low density hydrogen discharge.

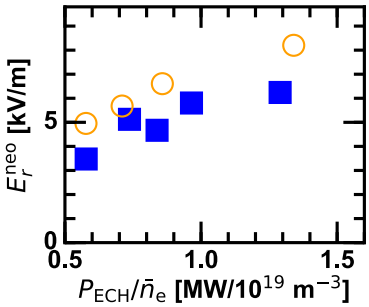

Figure 7. Numerically predicted neoclassical ambipolar radial electric field in the ECH applied phase.

dependence of the ITB threshold. Note that the threshold value in $P_{ECH}/\bar{n}_e$ is not perfectly identical to the case shown in Fig. 1 due to different experimental conditions.

Discussion

Since the neoclassical E_r transition plays a role for the ITB criticality,[14–17] whether neoclassical E_r has a susceptibility to the plasma ion mass is numerically examined by a local neoclassical transport code DKES/PENTA.[22] Figure 7 shows the $P_{ECH}/\bar{n}_e$ dependence of calculated neoclassical E_r at $r_{eff} \sim 0.2$ m in the ECH applied phase. Although neoclassical E_r is systematically larger in D plasmas in the electron-root solution, critical behavior is visible neither in D nor H plasmas. This examination implies that other mechanisms rather than the simple local neoclassical theory are necessary for explaining the isotope effect in the ITB threshold. Zonal flows[20] having an isotopic mass dependence[23] would be a candidate as the underlying mechanism. Global neoclassical effects are also important particularly close to the magnetic axis, which is dependent on the ion gyroradius.

An extra input power necessary for the E_r structure formation at the high-confinement mode transition in hydrogen plasmas is reported in the ASDEX-Upgrade tokamak,[8] which possibly has a link to the present case. In addition, an important role of the fast ions produced by NBs on core transport suppression is recently shown to have an isotope effect,[24] which can also contribute to the isotope effect in the ITB criticality.

Summary

In conclusion, the isotope effect in the electron ITB threshold favorable to plasmas with heavier ions was found. The radial electric field structure likely responsible for the ITB formation was easily formed in plasmas with heavier ions. A better core plasma performance with ITB in future deuterium-tritium plasmas is therefore foreseen. Transport barrier structures are regarded as a dissipative structure formed spontaneously in nonequilibrium open system by an intensive power input.[25] The present work also contributes to understanding of the dissipative structure affected by basic properties of the media.

Methods

Large Helical Device (LHD)

LHD is a plasma current-free magnetically confined torus plasma device. High-temperature plasmas are confined in the externally excited helical magnetic field structure with the toroidal magnetic field of $B_t = 2.75$ T and the vacuum torus axis of $R = 3.6$ m. In the vacuum magnetic field configuration, the rotational transform, $\iota/2\pi = 1/q$, where q is the safety factor, monotonically increases with the radius. The rational surfaces of $\iota/2\pi = 0.5$ and 1 typically exist at the core and the edge, respectively. In the present experiments, the plasma is sustained by balanced tangential neutral beams (NBs) with $P_{NB} = 3.6$ MW. The deuterium content is determined as $I_{D_\alpha}/(I_{D_\alpha} + I_{H_\alpha})$, where I_{D_α} and I_{H_α} are the intensities of the D_α emission and the H_α emission measured by a passive spectroscopy, respectively.

Heavy Ion Beam Probe (HIBP)

HIBP provides a direct measurement of the plasma electrostatic potential.[18] Heavy ion beam injected to the plasma is secondary ionized, where the beam trajectory diverges from the original beam trajectory. A part of the secondary ionized beam is selected by a slit, and the beam energy is analyzed. The energy difference between the original beam and the secondary ionized beam is equivalent to the electrostatic potential at which the secondary ionization occurs. To manipulate the measurement location, operational parameters for the HIBP, such as the injection beam energy, the incident angle, and the confinement magnetic field, are chosen according to the result of the beam trajectory calculation.

References

1. Bessenrodt-Weberpals, M. *et al.* The isotope effect in ASDEX. *Nucl. Fusion* **33**, 1205 (1993).
2. Hawryluk, R. J. Results from deuterium-tritium tokamak confinement experiments. *Rev. Mod. Phys.* **70**, 537 (1998).
3. Cordey, J. G. *et al.* Plasma confinement in JET H mode plasmas with H, D, DT and T isotopes. *Nucl. Fusion* **39**, 301 (1999).
4. Maggi, C. F. *et al.* Isotope effects on LH threshold and confinement in tokamak plasmas. *Plasma Phys. Control. Fusion* **60**, 014045 (2018).
5. Yamada, H. *et al.* Isotope Effect on Energy Confinement Time and Thermal Transport in Neutral-Beam-Heated Stellarator-Heliotron Plasmas. *Phys. Rev. Lett.* **123**, 185001 (2019).
6. Yan, Z. *et al.* Turbulence and sheared flow structures behind the isotopic dependence of the LH power threshold on DIII-D. *Nucl. Fusion* **57**, 126015 (2017).
7. Plank, U. *et al.* H-mode power threshold studies in mixed ion species plasmas at ASDEX Upgrade. *Nucl. Fusion* **60**, 074001 (2020).
8. Cavedon, M. *et al.* Connecting the global H-mode power threshold to the local radial electric field at ASDEX Upgrade. *Nucl. Fusion* **60**, 066026 (2020).
9. Kobayashi, T. *et al.* Isotope effects in self-organization of internal transport barrier and concomitant edge confinement degradation in steady-state LHD plasmas. *Sci. Rep.* **9**, 15913 (2019).
10. Kobayashi, T. The physics of the mean and oscillating radial electric field in the L–H transition: the driving nature and turbulent transport suppression mechanism. *Nucl. Fusion* **60**, 095001 (2020).
11. Yamada, I. *et al.* Recent progress of the LHD Thomson scattering system. *Fus. Sci. Technol.* **58**, 345–351 (2010).
12. Kobayashi, T. *et al.* Isotope effect in transient electron thermal transport property and its impact on the electron internal transport barrier formation in LHD. *Nucl. Fusion* **60**, 076015 (2020).
13. Yamada, H. *et al.* Characterization of energy confinement in net-current free plasmas using the extended International Stellarator Database. *Nucl. Fusion* **45**, 1684 (2005).

14. Fujisawa, A. *et al.* Electron thermal transport barrier and density fluctuation reduction in a toroidal helical plasma. *Phys. Rev. Lett.* **82**, 2669 (1999).

15. Stroth, U. *et al.* Internal transport barrier triggered by neoclassical transport in W7-AS. *Phys. Rev. Lett.* **86**, 5910 (2001).

16. Estrada, T. *et al.* Electron internal transport barrier formation and dynamics in the plasma core of the TJ-II stellarator. *Plasma Phys. Control. Fusion* **46**, 277 (2003).

17. Ida, K. *et al.* Characteristics of electron heat transport of plasma with an electron internal-transport barrier in the large helical device. *Phys. Rev. Lett.* **91**, 085003 (2003).

18. Ido, T. *et al.* 6 MeV heavy ion beam probe on the Large Helical Device. *Rev. Sci. Instrum.* **77**, 10F523 (2006).

19. Kobayashi, T. *et al.* Reconstruction of high temporal resolution Thomson scattering data during a modulated electron cyclotron resonance heating using conditional averaging. *Rev. Sci. Instrum.* **87**, 043505 (2016).

20. Itoh, K. *et al.* Physics of internal transport barrier of toroidal helical plasmas. *Phys. Plasmas* **14**, 020702 (2007).

21. Xu, Y. *et al.* Isotope effect and multiscale physics in fusion plasmas. *Physical review letters* **110**, 265005 (2013).

22. Spong, D. A. Generation and damping of neoclassical plasma flows in stellarators. *Phys. Plasmas* **12**, 056114 (2005).

23. Hahm, T. S. *et al.* Isotopic dependence of residual zonal flows. *Nucl. Fusion* **53**, 072002 (2013).

24. Schneider, P. A. *et al.* Fast-ion pressure dominating the mass dependence of the core heat transport in ASDEX Upgrade H-modes. *Nucl. Fusion* **61**, 036033 (2021).

25. Razumova, K. A. *et al.* Tokamak plasma self-organization-synergetics of magnetic trap plasmas. *Nucl. Fusion* **51**, 083024 (2011).

Acknowledgement

The authors thank the LHD experiment group for their assistance, and S. Sakakibara, M. Osakabe, T. Morisaki, H. Yamada, and K. Tanaka for strong support. This work is partly supported by JSPS Core-to-Core Program, A. Advanced Research Networks (PLADyS) and JSPS Grant-in-Aid for Scientific Research (17K14898, 18K03589, and 21K13902).

Author contributions

T.K, A.S, M.N, T.I, T.T, T.I.T, K.N and K.I. performed the experiment. S.S. provided the simulation data. T.K. analyzed the data. T.K. wrote the main manuscript text and all authors reviewed the manuscript.

Additional Information

Competing Interests: The authors declare that they have no competing interests.